Published in final edited form as:

Biochemistry. 2015 May 19; 54(19): 2943–2956. doi:10.1021/acs.biochem.5b00292.

The fibril core of transforming growth factor beta-induced protein (TGFBIp) facilitates aggregation of corneal TGFBIp

Charlotte S. Sørensen[1,¶,+], **Kasper Runager**[1,¶,§], **Carsten Scavenius**[§], **Morten M. Jensen**[§], **Nadia S. Nielsen**[+], **Gunna Christiansen**[Δ], **Steen V. Petersen**[Δ], **Henrik Karring**[$], **Kristian W. Sanggaard**[¶,§], and **Jan J. Enghild**[*,¶,§]

[¶]Center for Insoluble Protein Structures, Aarhus University, Gustav Wieds vej 10C, DK-8000 Aarhus C, Denmark

[+]Interdisciplinary Nanoscience Center, Aarhus University, Gustav Wieds vej 10C, DK-8000 Aarhus C, Denmark

[§]Department of Molecular Biology and Genetics, Aarhus University, Gustav Wieds vej 10C, DK-8000 Aarhus C, Denmark

[Δ]Department of Biomedicine, Aarhus University, Wilhelm Meyers Allé 4, DK-8000 Aarhus C, Denmark

[$]Department of Chemical Engineering, Biotechnology and Environmental Technology, University of Southern Denmark, Niels Bohrs Allé 1, DK-5230 Odense M, Denmark

Abstract

Mutations in the transforming growth factor beta-induced (*TGFBI*) gene result in a group of hereditary diseases of the cornea that are collectively known as *TGFBI* corneal dystrophies. These mutations translate into amino acid substitutions mainly within the fourth fasciclin 1 domain (FAS1-4) of the transforming growth factor beta-induced protein (TGFBIp) and cause either amyloid or non-amyloid protein aggregates in the anterior and central parts of the cornea, depending on the mutation. The A546T substitution in TGFBIp causes lattice corneal dystrophy (LCD), which manifests as amyloid-type aggregates in the corneal stroma. We previously showed that the A546T substitution renders TGFBIp and the FAS1-4 domain thermodynamically less stable compared with the wild-type (WT) protein, and the mutant FAS1-4 is prone to amyloid formation *in vitro*. In the present study, we identified the core of A546T FAS1-4 amyloid fibrils. Significantly, we identified the Y571-R588 region of TGFBIp, which we previously found to be enriched in amyloid deposits in LCD patients. We further found that the Y571-R588 peptide seeded fibrillation of A546T FAS1-4 and, more importantly, we demonstrated that native TGFBIp aggregates in the presence of fibrils formed by the core peptide. Collectively, these data suggest an involvement of the Y571-R588 peptide in LCD pathophysiology.

[*]Corresponding author: Jan J. Enghild, Department of Molecular Biology and Genetics, Aarhus University, 8000 Aarhus C, Denmark. Tel: +45 87155449 jje@mb.au.dk.

[1]The first two authors contributed equally to this work.

The authors have no competing financial interests.

Transforming growth factor beta-induced protein (TGFBIp, also called keratoepithelin) is an extracellular matrix protein that is expressed in a wide range of tissues at high levels in skin, bone, kidney and cornea [1–4]. Mutations in the transforming growth factor beta-induced (*TGFBI*) gene are associated with several autosomal dominant corneal dystrophies that are characterized by progressive accumulation of proteinaceous aggregates in the cornea. These dystrophies include lattice corneal dystrophies (LCDs), which are defined by the formation of amyloid fibrils in the sub-epithelial anterior and central parts of the cornea, and granular corneal dystrophies (GCDs), which are characterized by the deposition of opacities in the corneal stroma [5]. The only available treatments of *TGFBI* corneal dystrophies are lamellar keratoplasty or phototherapeutic keratectomy for disorders that only affect the superficial cornea; full-thickness corneal transplant can be used in severe cases with TGFBIp deposits throughout the corneal stroma [6–9]. However, the impact of these treatments is normally transient because there is a risk of new protein accumulation in the donor cornea [10–12]. Moreover, donor corneas may be scarce. Therefore there is an urgent need for alternative, less invasive treatments.

Amyloid fibrils are self-assembled protein structures that are associated with corneal dystrophies and several neurodegenerative diseases including Alzheimer's disease and Parkinson's disease [13]. Amyloids are generally extremely stable structures with a fibril core that is comprised mainly of beta-sheet secondary structure elements [14]. This beta-rich core is essential to the thermodynamic stability of the fibril. Therefore, this core is an attractive target for therapeutic intervention in amyloid diseases.

Previous attempts to localize the fibril core of amyloidogenic TGFBIp mutants have analyzed the aggregation propensity of synthetic peptides representing regions from TGFBIp predicted to be prone to fibrillation [15, 16]. These peptides covered regions in the termini of the fourth fasciclin 1 domain (FAS1-4) of TGFBIp, specifically F515-N532 and E611-Q633.

The present study characterized the fibril structure that is induced by the naturally occurring A546T mutation in TGFBIp. The A546T mutation produces an LCD variant (previously known as LCD IIIa) that manifests as thick, ropy lattice lines throughout the stroma and causes corneal erosions; this phenotype corresponds to an autosomal dominant inheritance pattern [17, 18]. Our recent study showed that mutations in FAS1-4 affect the thermodynamic stability of TGFBIp and the A546T mutation drives the FAS1-4 domain towards the formation of amyloid fibrils via structural destabilization [19]. Here, we identify the segment that constitutes the fibril core of A546T FAS1-4 amyloid fibrils. The region identified contained the Y571-R588 segment, which we recently showed was enriched in LCD corneal deposits [20–22]. We further demonstrated that fibrils of the core peptide induced fibrillation of A546T FAS1-4 and caused aggregation of native WT TGFBIp in corneal protein extracts. Consistent with our previous identification of the Y571-R588 peptide in LCD corneal deposits, our findings indicate that this peptide plays a central role in LCD pathogenesis.

EXPERIMENTAL PROCEDURES

Materials

Unless otherwise stated, chemicals were from Sigma-Aldrich Co. (St. Louis, MO, USA). The F515-R533 and Y571-R588 peptides were synthesized at EZBiolab Inc. (Carmel, IN, USA). Professor Daniel Otzen, Aarhus University, kindly provided α-synuclein fibrils. A healthy eye was obtained post-mortem from an 86-year-old male at Aarhus University Hospital, and it was collected within 48 h after time of death.

Cloning, expression, and purification of mutant A546T FAS1-4 and WT TGFBIp

An A546T FAS1-4 construct encoding amino acid residues 502–657 from human TGFBIp (SwissProt accession number Q15582) plus two additional N-terminal amino acid residues (denoted A500' and G501') was cloned, expressed and purified as previously described [19]. WT TGFBIp was also cloned, expressed and purified as previously described [23], with minor modifications in cell type and the transfection protocol. Expression was induced in the human cell line Freestyle 293-F (Invitrogen, Madison, WI, USA) using the polyethylenimine transfection method [24]. Purified proteins were dialyzed against phosphate-buffered saline (PBS) (20 mM sodium phosphate, 137 mM NaCl, pH 7.4), frozen in liquid nitrogen and stored at −80°C.

Sodium dodecyl sulfate-polyacrylamide gel electrophoresis (SDS-PAGE)

Protein fragments of the insoluble and soluble fractions of monomeric and fibrillated A546T FAS1-4 before and after trypsin digestion were separated in 10–15% polyacrylamide gels using SDS-PAGE [25]. DTT (35 mM) and SDS (1%) were added to prepare the samples for electrophoresis, and the samples were boiled for 5 min. After separation, the gel was stained with Coomassie brilliant blue. Bands of interest were analyzed using N-terminal sequencing on a separate gel.

N-terminal sequencing

Reversed-phase HPLC (RP-HPLC) fractions were applied directly to micro trifluoroacetic acid (TFA) filters and sequenced using automated Edman degradation (PROCISE TM 494 HT sequencer with on-line phenylthiohydantoin analysis by HPLC, Applied Biosystems, Foster City, CA, USA). Proteins were electrophoretically transferred to a polyvinylidene fluoride (PVDF) membrane (Millipore, Billerica, MA, USA) in 10 mM N-cyclohexyl-3-aminopropanesulfonic acid (CAPS), 10% (v/v) methanol, pH 11, as described previously [26], to sequence the N-termini of the SDS-PAGE-separated proteins. Subsequently, the bands of interest were excised and analyzed.

Matrix-assisted laser desorption/ionization time-of-flight (MALDI-TOF) mass spectrometry

Samples from RP-HPLC were lyophilized and mixed 1:1 v/v with α-cyano-4-hydroxycinnamic acid in 70% acetonitrile and 0.1% TFA and spotted directly onto the MALDI target. The analysis of peptides larger than 4,000 Da was performed on an Autoflex III smart-beam instrument (Bruker, Billerica, MA, USA), and peptides with masses below

4,000 Da were analyzed using a Q-TOF Ultima MALDI mass spectrometer (Waters Corporation, Milford, MA, USA).

Fibrillation of A546T FAS1-4 and synthetic peptides

Proteinase inhibitors (cOmplete Proteinase inhibitor cocktail - EDTA free, Roche Diagnostics, Basel, Switzerland), sodium azide (0.02%) and EDTA (5 mM) were added to all samples in order to prevent bacterial growth and adventitious proteolysis during fibrillation. The recombinant A546T FAS1-4 protein (1.2 mg/ml in PBS) and synthetic F515-R533 and Y571-R588 peptides, which were used for the seeded fibrillation assay and pull-down experiments described below, were fibrillated in a thermoshaker (Grant Bio, Hillsborough, NJ, USA) for 8 days (A546T FAS1-4) or 4 days (peptides) at 37°C with shaking at 900 rpm. The synthetic F515-R533 and Y571-R588 peptides were dissolved in dimethyl sulfoxide (DMSO) at a concentration of 4.3 mM and diluted to 43 μM in PBS before fibrillation. In experiments where the two peptides were mixed, the concentration of each peptide was also 43 μM and in seeding experiments seeds of the peptides were produced separately and only mixed when added to the A546T FAS1-4. A546T FAS1-4 was fibrillated at a concentration of 0.3 mg/mL, and 10 or 20% (molar ratio) core peptide seeds were added, when testing the ability of fibrillated F515-R533 and Y571-R588 to seed the fibrillation of A546T FAS1-4. The seeds were obtained using sonication of F515-R533 and Y571-R588 fibrils at 30% amplitude for 3 × 10 s (Labsonic M, Sartorius, Goettingen, Germany). Thioflavin T (ThT) was added to a final concentration of 40 μM to visualize the fibrillation process, and the samples were incubated in a 96-well plate at 37°C in a plate reader (FLUOstar Omega, BMG LABTECH, Ortenberg, Germany). The fibrillation of the core peptides was performed in optical bottom surface- coated polystyrene plates (Cat#: 165305, Thermo Scientific, Waltham, MA, USA), and the seeded fibrillation assays were carried out in optical bottom polystyrene plates (Cat#: 3631, Corning, New York, NY, USA). The samples were set up for fibrillation with double orbital shaking for 2 min at 500 rpm every 20 min. The excitation wavelength was 450 nm, and emission was measured at 485 nm. The fibrillations were performed in triplicate. Monitoring of ThT binding to fibril seeds was performed in duplicates.

Hydrogen-Deuterium Exchange Mass Spectrometry (HDX-MS)

Automatic sample handling, online proteolysis and LC/MS analysis of the deuterated samples were performed using a H/D-X PAL system (LEAP Technologies, Carrboro, NC, USA) coupled to an Ultimate 3000 UPLC system (Dionex, Sunnyvale, CA, USA) and an Ultima Q-TOF mass spectrometer (Micromass/Waters, Milford, MA, USA). The fibrillated A546T FAS1-4 was isolated as a pellet via centrifugation at 16,100 × *g* for 15 min, followed by washing in PBS to remove excess monomeric A546T FAS1-4 that was loosely associated with the pellet. Monomeric or fibrillated A546T FAS1-4 was allowed to undergo hydrogen-deuterium exchange in a 87% deuterated buffer containing 10 mM Tris-HCl and 137 mM NaCl at pD 7.4 for increasing time intervals (30 sec, 2 min, 5 min, 10 min, 30 min 60 min, 3 h, 12 h and 72 h) at 2°C. A fully deuterated FAS1-4 sample was generated by incubating monomeric FAS1-4 in the deuteration buffer for 1 h at 95°C 24 h followed by 23 h at 2°C. Deuterium uptake was quenched, and the fibrils were solubilized in 6 M urea and 300 mM glycine pH 2.5 at 4°C for 1 min, after which time the samples were diluted 3-fold with 0.1%

formic acid. The quenched samples were injected onto a 2 × 40 mm column packed with immobilized pepsin (POROS AL 20 Applied Biosystems, Foster City, CA, USA) followed by desalting on a UPLC reversed-phase trap column (ACQUITY UPLC BEH 130 Å C18 1.7 μm, 2.1×5 mm, VanGuard Pre-column, Waters, Milford, MA, USA). Digestion, trapping and desalting were performed using a 0.1% formic acid solution at 0.2 ml/min for 2 min. The peptides were eluted from the pre-column and separated by RP-HPLC (ACQUITY UPLC BEH C18 1.7 μm 1.0 × 100 mm) using a gradient of buffer A (0.1% formic acid) and buffer B (90% acetonitrile + 0.1% formic acid) from 10% B to 45% B in 10 min and 45% B to 95% B in 1 min followed by 5 min of 95% B at a flow rate of 40 μL/min. The Q-TOF Ultima mass spectrometer was operated with a capillary voltage of 3.5 kV, cone voltage of 35 V, source temperature at 80°C and desolvation temperature at 150°C. The scan range was set to *m/z* 250–1800 with a scan time of 1 sec. Retention times and identity of the pepsin-generated peptides were obtained via LC-MS/MS analyses of non-labeled samples using identical chromatographic conditions. The raw data were converted into peak lists and searched using a local MASCOT search engine. The deuterium uptake level was calculated using HDExaminer software (Sierra Analytics, Modesto, CA, USA), and it was based on all charged species of the LC-MS/MS-identified peptides. Results from the fully deuterated sample were used to calculate the back-exchange occurring during quench, fibril dissociation, on-line pepsin digestion and LC/MS analysis. All peptides in the partially deuterated samples were corrected for back-exchange based on the back-exchange observed in the fully deuterated sample [27]. A representative data set from 3 individual experiments is shown.

Identification of the fibril core using proteolysis and transmission electron microscopy (TEM)

Monomeric and fibrillated A546T FAS1-4 were separated into insoluble and soluble fractions using centrifugation at 16,100 × *g* for 15 min. The concentration of fibrillated A546T FAS1-4 was determined via fibrillation of a known amount and subsequent analysis of the supernatant and pellet using SDS-PAGE. The protein amount in the pellet and supernatant was evaluated using visual inspection of the Coomassie-stained gel. The insoluble fraction was washed in PBS. The supernatant from the monomeric A546T FAS1-4 sample, containing the majority of the protein amount, was incubated with trypsin at a ratio of 1:1 w/w at 37°C for two h, and the trypsin was inhibited with 2 mM phenylmethane-sulfonylfluoride (PMSF) for 30 min at 23°C. The digest was separated into insoluble and soluble fractions via centrifugation. The insoluble fraction of fibrillated A546T FAS1-4 was resuspended in PBS and subjected to proteolysis and centrifugation following the same procedure as monomeric A546T FAS1-4. Fibrillated samples before and after proteolysis were visualized using TEM. Prior to TEM, 150 μL of fibrillated material was isolated as a pellet via centrifugation and resuspended in 20 μL PBS. The concentrated samples (5 μL) were placed on 400-mesh carbon-coated, glow discharged Ni grids for 30 s, washed with distilled water and stained with 1% phosphotungstic acid (pH 6.8). A Jeol 1010 transmission electron microscope (JEOL Tokyo, Japan) equipped with an Olympus KeenView TEM CCD camera system (Olympus Soft Imaging Solutions GMBH, Münster, Germany) was used to visualize the fibrillated material.

Fractionation of soluble and insoluble protein fragments using RP-HPLC

Supernatant and pellet fractions obtained after trypsin digestion of fibrillated A546T FAS1-4 were analyzed and separated using RP-HPLC. The insoluble fraction was washed in PBS and dissolved in 6 M guanidine hydrochloride for 5 min. Samples were acidified via the addition of 0.1% TFA and applied to a reversed-phase column (Vydac C18 2.1 mm, Phenomenex, Torrance, CA, USA), followed by washing of the column in approximately 5 × column volumes of solvent A (0.1% TFA). The samples were eluted from the column with a linear gradient from solvent A to 90% solvent B (90% acetonitrile, 0.07% TFA) at 1% B/min. All peaks from the insoluble samples were collected manually. Fractions were lyophilized and analyzed using N-terminal sequencing and mass spectrometry (peptides with masses larger than 4,000 Da were analyzed on an Autoflex III smart-beam instrument and peptides with masses below 4,000 Da were analyzed using a Q-TOF Ultima MALDI mass spectrometer).

Formation and identification of fibrillating peptides derived from A546T FAS1-4

The purified, monomeric A546T FAS1-4 protein was digested with trypsin, at a A546T FAS1-4:trypsin ratio of 20:1 (w:w), for 4 h at 37°C. Protease inhibitors, sodium azide and ThT were then added, and the sample was incubated in a plate reader, as described above. Following fibrillation the aggregates, in a parallel sample without ThT, were isolated via centrifugation, and the peptides were separated using RP-HPLC, as described above. Finally, the separated peptides were identified using N-terminal sequencing and mass spectrometry (Q-TOF Ultima MALDI mass spectrometer).

Preparation of natively extracted human corneal proteins

The eye was rinsed in isotonic saline immediately after removal, and the clearness of the cornea was inspected under a dissection microscope. The eye was stored at −80°C until further use. The eye was thawed, and the corneal epithelium was removed by washing with 70% ethanol and gentle scraping using a surgical blade. The remaining part of the cornea was carefully excised to avoid the corneal limbus and washed briefly in water. The endothelium was removed in the same manner as the epithelium. The corneal stroma was stored at −80°C until further use. After thawing, the corneal stroma was cut into smaller pieces, lyophilized and homogenized (IKA Werke Ultra-Turrax T8, Staufen, Germany) in liquid nitrogen, dissolved in 2 ml of extraction buffer (1 M $(NH_4)_2SO_4$, 50 mM Tris-HCl, pH 7.4, 5 mM EDTA and cOmplete Proteinase inhibitor cocktail – EDTA-free) and incubated for 4 h at 4°C while rotating. The sample was centrifuged for 20 min at 2,500 × *g* at 4°C to remove the insoluble fraction and dialyzed into tris-buffered saline (TBS) (137 mM NaCl, 20 mM Tris-HCl, pH 7.4) with 1 mM $CaCl_2$. Finally, the protein concentration was determined using absorbance readings at 280 nm (NanoDrop2000 Spectrophotometer, Thermo Scientific, Waltham, MA, USA).

Fibril-based pull-down assays

The corneal stroma extract and purified TGFBIp were centrifuged at 40,000 × *g* at 4°C for 15 min and filtered through centrifugal filters with a pore size of 0.45 μm (VWR, Radnor, PA, USA) to remove any preformed aggregates. The fibrillated samples (A546T FAS1-4, α-

synuclein, and synthetic peptides) were centrifuged at 40,000 × *g* at 4°C for 15 min (Sorvall Evolution RC centrifuge, Kendro, Newton, CT, USA) to collect the fibrils. Corneal stroma extract (11.25 μg total protein) was incubated with 15 μg of either fibrillated A546T FAS1-4, F515-R533, Y571-R588, or α-synuclein or without fibrils for 18 h at 4°C while shaking at 500 rpm. Similarly, 10 μg of recombinant TGFBIp was incubated with 10 μg of fibrillated material or without fibrils. The solution was transferred to a 0.45 μm centrifugal filter and the supernatant was centrifuged through the filter at 1,000 × *g* for 4 min to isolate the fibrils on top of the filter. The filters were rinsed three times with TBS and subsequently washed for 30 min with 1 M NaCl, 20 mM Tris-HCl, and 5 mM EDTA, pH 7.4. Each washing step was followed by centrifugation to remove the buffer. Incubation with 6 M guanidine hydrochloride for 30 min at 23°C dissolved the isolated fibrils, and subsequent centrifugation isolated the dissolved fibrils and associated proteins. The samples were desalted using micropurification [28] and subjected to SDS-PAGE analysis. Western blotting (corneal stromal extract) or Coomassie brilliant blue staining (recombinant TGFBIp) was subsequently used to visualize the proteins resolved by SDS-PAGE. Western blotting was performed using a polyclonal antibody against full-length TGFBIp [29, 30] and a Cy3-labeled secondary antibody (Sigma-Aldrich Co., St. Louis, MO, USA). Proteins were visualized using a fluorescence scanner (FluorChem Q, ProteinSimple, Santa Clara, CA, USA) and AlphaView software (ProteinSimple, Santa Clara, CA, USA). All samples were analyzed in triplicate and normalized to a loading control using the same fluorescence scanner and software described above for quantification. Student's t-tests were performed to compare the quantitations.

RESULTS

HDX-MS reveals the core of A546T FAS1-4 amyloid fibrils

We previously demonstrated that full-length A546T TGFBIp and A546T FAS1-4 mutants are both destabilized compared with WT proteins, and the A546T FAS1-4 domain has an increased propensity to form amyloid fibrils [19, 31]. Consequently, we used A546T FAS1-4 as a model system to characterize the structure and formation of TGFBIp amyloid fibrils. The formation of amyloid fibrils was achieved by mild shaking of A546T FAS1-4 in solution as described previously [19, 31]. We compared the hydrogen exchange dynamics of A546T FAS1-4 fibrils to monomeric protein using HDX-MS to probe the structure of A546T FAS1-4 fibrils (Fig. 1). This method exploits the fact that the hydrogen exchange rate of backbone amides is structure-dependent. In general, solvent shielding or participation in hydrogen bonds in secondary structural elements results in a slower exchange rate. Our data showed that the exchange of the backbone hydrogens in monomeric A546T FAS1-4 was fast, and most of the exchange occurred within 10 min. Fibrillated A546T FAS1-4 in general displayed reduced exchange, which suggests a higher degree of protection from the solvent and/or stabilized secondary structure elements. The peptides covering the region L565-L597 (numbered according to the full-length TGFBIp precursor including the signal peptide) in fibrillated A546T FAS1-4 showed a low exchange rate (less than 40%) compared with the monomeric sample. The regions A500'-Y537 and E598-T629 also displayed decreased exchange in the fibrillated sample compared with the monomeric sample, however to a less degree than the L565-L597 region. To assess the resistance to hydrogen

exchange at a longer time scale we subjected the A546T FAS1-4 fibrils to an exchange period of 72 h in deuterated buffer (Fig. 2). During this time only a minor increase in the deuterium uptake was observed and the L565-L597 region still presented the highest degree of protection.

Collectively, the HDX-MS data suggested that the fibril core of A546T FAS1-4 is contained within the L565-L597 region, which implies that the mutated amino acid residue (A546T) is not part of the core region of the fibrils.

Two regions in A546T FAS1-4 fibrils are resistant to proteolysis

To narrow the region that is essential to amyloid stacking in A546T FAS1-4 fibrils we took advantage of the tight packing within amyloid fibrils, which renders the protein backbone less susceptible to proteolysis (Fig. 3). We used the proteinase trypsin for this purpose because it reliably produces protein fragments of defined sizes that are suitable for downstream analyses. Fibrillated A546T FAS1-4 was incubated with trypsin to generate fibril core-containing fragments. Supernatants and pellets were separated using centrifugation and analyzed using SDS-PAGE and TEM. Monomeric A546T FAS1-4 and fibrils that were not treated with trypsin were included as controls (Fig. 3A). The analysis demonstrated that freshly purified monomeric A546T FAS1-4 was soluble and readily cleaved by trypsin. By contrast, trypsin proteolysis of the pellet from the fibrillated sample resulted in accumulation of insoluble A546T FAS1-4 fragments of defined sizes (Fig. 3A). TEM of untreated and trypsin-treated pellets confirmed the presence of fibrils (Fig. 3C and 3D), which indicates that part of the fibril structure was unaffected by trypsin treatment. N-terminal sequencing established the identity of 7–8 amino acid residues from the N-termini of the proteolysis-resistant insoluble fragments. The largest fragment, which migrated just below the 6.5-kDa marker (Fig. 3A, Band 1), represented two N-termini: L^{558}LGDAKEL^{565} and E^{564}LANILK^{570} (Fig. 3A and 3B). The signal from L^{558}LGDAKEL^{565} was the most intense (data not shown). Both N-termini correspond to the central region of A546T FAS1-4. The more faint band (Fig. 3A, Band 2), was found to contain the N-termini L^{558}LGDAKEL^{565} and $A^{500'}$GMGTVMD^{507}, and thus contained an N-terminal fragment of A546T FAS1-4 in addition to the central region.

The proteolytic peptides in the supernatant and pellet of the trypsin-treated A546T FAS1-4 fibrils were separated using RP-HPLC to determine the full sequence of the fibril core fragments (Fig. 4). Comparison of the elution profiles of the pellet and supernatant revealed four major and one minor peaks that were only present in the pellet (Fig. 4A, lower chromatogram, numbers 1–5). A combination of N-terminal sequencing and mass spectrometry established the identities of these peptides as overlapping fragments that contained 2–7 missed tryptic cleavages and covered two areas in A546T FAS1-4 (Figs. 4B and 4C). Collectively, the data showed that two regions were resistant to trypsin proteolysis: the most abundant species covered a central region E564-K602 while the less abundant species covered an N-terminal part of A546T FAS1-4 A500'-R533 (Fig. 4C). These two regions correlate well with the data obtained from HDX-MS and suggest the successful identification of the primary and secondary regions that constitute the fibril core.

Isolation and characterization of two highly amyloidogenic tryptic peptides in A546T FAS1-4

The two regions identified when analyzing the core of A546T FAS1-4 fibrils were relatively large, and we hypothesized that the regions that initiate fibril formation are considerably smaller. Monomeric A546T FAS1-4 was extensively digested with trypsin and incubated in a plate reader with shaking in the presence of ThT to identify the parts of the fibril core regions with the highest amyloidogenic capacity (data not shown). Once there was no further increase in fluorescence, the aggregated fraction of a parallel sample (without ThT) was isolated, and the peptides were separated using RP-HPLC (Fig. 5A). Subsequently, N-terminal sequencing and mass spectrometry were used to determine the identity of the peptides (Fig. 5B). The fibril pellet contained two A546T FAS1-4 tryptic peptides: F515-R533 and Y571-R588. A third peak containing a peptide was observed (Peak 2, Fig. 5B), but the N-termini therein were similar to the peptides in peaks 1 and 3. We could not identify any unique masses in peak 2 using mass spectrometry. This result suggests that this peak contains a modified peptide, or it is the result of a missed tryptic cleavage. The two identified peptides, F515-R533 and Y571-R588, mapped within the two fibril-forming regions that were identified by HDX-MS and limited proteolysis.

A combination of ThT fibrillation assays and electron microscopy was used to confirm the fibrillation propensities of the synthetic peptides Y571-R588 and F515-R533 (Fig. 6). The ThT assay showed that the exponential growth phase of F515-R533 started after 25 h of incubation (Fig. 6A), and the growth phase of Y571-R588 started after 15 h (Fig. 6C). When the two peptides were incubated together the lag phase was increased to approximately 30 h, while still maintaining a monophasic fibrillation curve (Fig. 6E). TEM images from the endpoints of all three experiments revealed linear fibrils that were regular in shape with many higher order structures (Figs. 6B and 6D). These results confirmed our hypothesis that the larger core regions identified by HDX-MS and proteolysis contained smaller regions, F515-R533 and Y571-R588, which were highly amyloidogenic.

Seeds of the fibril core peptides induce fibrillation of A546T FAS1-4

We showed that the F515-R533 and Y571-R588 peptides are likely encompassed in the core of TGFBIp fibrils. We next investigated the potential of these peptides to induce fibrillation of larger TGFBIp entities. We used seeds from mature peptide fibrils and tested their seeding capacities on A546T FAS1-4 using a ThT fluorescence assay (Fig. 7). Seeds of the fibril core peptides were incubated with A564T FAS1-4 either alone or in combination. In all cases a dose-dependent decrease in lag time was observed as the seed concentrations were increased (Fig. 7A–C). Specifically, an immediate increase in ThT fluorescence was observed when A546T FAS1-4 was incubated with increasing concentrations of F515-R533 seeds, while addition of Y571-R588 seeds resulted in a more gradual increase in ThT fluorescence. When A546T FAS1-4 was incubated with a combination of core peptide seeds there was an increased effect on seeding compared to the isolated core peptide seeds (Fig. 7C). Collectively, the seeding data suggest that both core peptides have the potential to seed fibrillation of A546T FAS1-4.

The fibril core peptides facilitate aggregation of TGFBIp

We extracted the soluble protein fraction from a human cornea and incubated it with fibrils of A546T FAS1-4 and core peptides to explore whether the fibril core peptides may play a role in the aggregation of TGFBIp *in vivo* (Fig. 8). Samples with and without fibrils of recombinant α-synuclein were included as controls. Washing the samples extensively using 1 M NaCl ensured that only proteins in large high-affinity complexes were retained in the sample, which was analyzed using SDS-PAGE followed by immunoblotting using antiserum against TGFBIp (Fig. 8A). The data showed that TGFBIp from corneal stromal extract had a high affinity for fibrillated core peptides (F515-R533 and Y571-R588) and A546T FAS1-4 fibrils (Fig. 8A). Approximately 3 times more TGFBIp was bound to fibrils of the core peptide Y571-R588 compared with F515-R533 (Fig. 8B). Only trace amounts of TGFBIp were present in the two negative control samples (Fig. 8A and 8B).

Purified recombinant TGFBIp was incubated with fibrils as described above to investigate whether the aggregation of TGFBIp depended on other corneal proteins. Incubation of recombinant TGFBIp with fibrils demonstrated that the fibrils had a similar effect on recombinant TGFBIp as corneal TGFBIp (Fig. 8C). A larger amount of TGFBIp was present in the control samples compared with the corneal extract. However, there was a significant difference compared with the samples that contained fibrillated A546T FAS1-4, F515-R533 and Y571-R588 (Fig. 8D). Fibrillated Y571-R588 bound approximately 1.6 times the amount of recombinant TGFBIp as F515-R533 (Fig. 8D).

DISCUSSION

The *TGFBI*-linked corneal disorders are a diverse group of diseases that are caused by more than 50 different mutations in the *TGFBI* gene and result in several phenotypes, which can be clustered into two groups, lattice corneal dystrophies and granular corneal dystrophies [32]. Little is known about the disease mechanism, and it is enigmatic that different mutations in a single protein cause aggregates of varying appearance, localization, and effects on surrounding tissues [5]. However, we and other investigators showed that the disease-causing TGFBIp-mutants exhibit different stabilities and degradation pattern, which suggests that these factors are related to the disease mechanism [33–38]. We further showed that the LCD-associated mutant A546T displayed decreased thermodynamic and proteolytic stabilities compared with WT TGFBIp, but the GCD-associated mutation R555W stabilized TGFBIp [19, 31, 39]. Our previous data demonstrated that the stability and fibrillation propensity of the FAS1-4 domain were similar to full-length TGFBIp, which supports the use of FAS1-4 as a model system for TGFBIp fibrillation [19, 31]. The present study took advantage of this commonality and characterized the amyloid fibril core formed by A546T FAS1-4.

We here characterized the fibril core of A546T FAS1-4 using several experimental approaches. HDX-MS data revealed that the region L565-L597 displayed the highest degree of protection from hydrogen/deuterium exchange in A546T FAS1-4 fibrils compared with monomeric A546T FAS1-4. Our data for the L565-L597 region showed a relatively high degree of deuterium uptake (approximately 40%) compared to what is usually expected for amyloid cores [40]. However, cases with a higher degree of exchange have been described for

amyloid fibrils [41], and importantly we found the deuterium level in the A546T FAS1-4 fibril core to be stable during prolonged incubation. Thus, the relatively high uptake of deuterium in the fibril core of A546T FAS1-4 likely results from a combination of fibril dynamics and structural characteristics where a maturation of the fibril core is propagated from the central parts of the fibrils towards the ends creating a heterogeneous structure with a more loose packing of the fibril near the fibril extremities [42]. Electron microscopy showed that the fibrils were short, which would increase the solvent exposure and produce more fibril ends where a monomer-fibril transitions could occur [43]. Similar results have previously been reported for the Aβ40 fibril, in which a 50% deuterium uptake was observed after 3 days incubation [44]. Thus, there is a large variation in molecular recycling observed between different fibrils. Collectively, the HDX-MS data, indicated that region L565-L597 was the most stable, while the regions A500'-Y537 and E598-T629 were less protected against exchange.

Limited proteolysis of fibrillated A546T FAS1-4 provided complementary information about the dynamic nature of the polypeptide chain. The results further supported the involvement of the central region of FAS1-4 in the fibril core but additionally suggested that part of the N-terminal region A500'-R533 is buried in the fibril structure (Fig. 9). The fact that this region only showed medium degree of protection (~70%) in the HDX-MS data and was a minor species in the proteolysis data suggest that it is either less stable or that it only takes part in a fraction of the mature A546T FAS1-4 fibrils. Thus, the proteolysis data showed that the N-terminal region, which displayed a relatively high degree of deuterium exchange in the fibril, was relatively stable and may be involved in the fibril core.

To evaluate amyloidogenic potential across the A564T FAS1-4 sequence the domain was extensively digested with trypsin and peptides were subsequently allowed to fibrillate (Fig. 4). The presence of two amyloidogenic regions was confirmed, and collectively, the data suggested that these two TGFBIp-regions (F515-R533 and Y571-R588) contained the fibril core of A546T FAS1-4 and TGFBIp.

Comparisons of these results to those of previously reported fibril core studies revealed that the F515-R533 region overlapped with the F515-N532 region, which was previously described as highly amyloidogenic [15]. Significantly, our previous analyses of amyloid deposits in the cornea showed that the F515-R533 region was highly proteolytically processed compared with healthy controls, which suggested that this peptide was not part of the mature fibrils [20–22]. However, the involvement of the F515-R533 region in the early phases of fibril formation *in vivo* cannot be excluded. By contrast, the Y571-R588 region was previously observed in diseased corneal tissue [20–22]. Notably, this region accumulated in all of these LCD cases, which indicates that the mechanism of fibril core formation is independent of the mutation and the position of the mutation.

To elucidate the mechanism of TGFBIp aggregation *in vivo*, we investigated the ability of fibrils that were formed by the fibril core peptides to induce fibrillation of larger TGFBIp entities (Fig. 7). Both of the core peptides exhibited a dose dependent increase in seeding capacity, although the F515-R533 peptide gave a more immediate response than the Y571-

R588 peptide. Notably, the combination of the two core peptides considerably enhanced this effect, which suggests a cooperative seeding effect of these two peptides.

Having demonstrated that the core peptides seeded the fibrillation of an isolated TGFBIp domain, we next tested this effect in an '*in vivo*-like' situation using human corneal extract and isolated TGFBIp (Fig. 8). Our data showed that native TGFBIp from human corneal stroma and purified recombinant TGFBIp both aggregated when incubated with the amyloid fibrils formed by the core peptides (F515-R533 and Y571-R588), as well as A546T FAS1-4. The largest effect was again observed for the fibrillated Y571-R588 peptide compared with the fibrillated form of the other peptide. There was little to no aggregation with the negative control α-synuclein. These results suggest that fibril-induced TGFBIp aggregation/interaction depends on the amino acid sequence and/or structural determinants as opposed to non-specific interactions with fibrillated protein material in general. Moreover, the affinity was demonstrated to be independent from other components of the corneal extract because the same results were observed using purified recombinant TGFBIp. Combining these data with our observation that the core peptides seeded the fibrillation of A564T FAS1-4 indicate that the accumulating Y571-R588 region also binds or induces aggregation of full-length TGFBIp, which may promote the progressive nature of the disease and cause corneal haziness. The adsorbed TGFBIp might be directly incorporated into the amyloid structure or cause concentration-dependent precipitation. Both scenarios would likely lead to an increase in plaque volume and augment visual impairment. Therefore the present data suggest that the accumulating amyloid fibrils exert a self-perpetuating effect on plaque propagation. The accumulation of amyloid fibrils composed of peptides covering Y571-R588 in the cornea could occur as a result of endogenous proteolytic activity in an attempt to remove the TGFBIp fibrils. Alternatively, fibrils may arise when soluble TGFBIp is cleaved by proteases as part of the natural protein turnover mechanism, which in turn may be influenced by the stability changes of TGFBIp induced by the mutations. This event could release fibrillating peptides that cover the core regions, which might initiate fibrillation.

The data presented here suggest that the region Y571-R588 of TGFBIp may be a therapeutic target against LCD. Targeting the fibril core in amyloid disease was attempted previously using diverse approaches including the addition of bulky groups to the core peptide, replacement of a residue with proline, grafting of the peptide segment into the complementarity-determining region of antibodies, and N-methylation of the peptide backbone [15, 45–51]. These methods were effective *in vitro*, but they have not been implemented *in vivo*. We propose that any of these strategies may be applied to the fibril core peptides of TGFBIp to obtain an inhibitor of TGFBIp fibrillation. Additionally, the fibril core peptide Y571-R588 may be used as a model for TGFBIp fibrillation in high-throughput screenings of small-molecule fibril inhibitors.

In conclusion, we showed that A546T FAS1-4 formed amyloid fibrils with a primary and a secondary core region *in vitro*, and that both of these regions were highly amyloidogenic. The primary region (Y571-R588) accumulates in LCD corneas [20–22], and we showed that this region induced fibrillation of A546T FAS1-4 and facilitated the aggregation of TGFBIp. Mechanistically, we propose that this property may exacerbate the TGFBIp-related LCDs,

and the Y571-R588 region of TGFBIp may be a potential therapeutic target in TGFBIp-related LCDs.

Acknowledgments

We thank the laboratory of Professor Daniel Otzen, Aarhus University, who kindly provided fibrillated α-synuclein.

Funding

This work was supported by the National Eye Institute (R01 EY012712), The Danish Council for Independent Research – Medical Sciences (DFF - 4004–00471), The Lundbeck Foundation (R164-2013-15912), the Carlsberg Foundation, the Danish National Research Foundation (inSPIN) and Maskinfabrikant Jochum Jensen og hustru Mette Marie Jensen f. Poulsens Mindelegat.

ABBREVIATIONS

FAS1	fasciclin 1 domain
FAS1-4	the fourth fasciclin 1 domain
GCD	granular corneal dystrophy
HDX-MS	hydrogen deuterium exchange mass spectrometry
LCD	lattice corneal dystrophy
RP-HPLC	reversed-phase HPLC
TEM	transmission electron microscopy
TGFBI	transforming growth factor beta-induced
TGFBIp	transforming growth factor beta-induced protein
ThT	thioflavin T

REFERENCES

1. LeBaron RG, Bezverkov KI, Zimber MP, Pavelec R, Skonier J, Purchio AF. Beta IG-H3, a novel secretory protein inducible by transforming growth factor-beta, is present in normal skin and promotes the adhesion and spreading of dermal fibroblasts in vitro. The Journal of investigative dermatology. 1995; 104:844–849. [PubMed: 7738366]
2. Kitahama S, Gibson MA, Hatzinikolas G, Hay S, Kuliwaba JL, Evdokiou A, Atkins GJ, Findlay DM. Expression of fibrillins and other microfibril-associated proteins in human bone and osteoblast-like cells. Bone. 2000; 27:61–67. [PubMed: 10865210]
3. Lee SH, Bae JS, Park SH, Lee BH, Park RW, Choi JY, Park JY, Ha SW, Kim YL, Kwon TH, Kim IS. Expression of TGF-beta-induced matrix protein betaig-h3 is up-regulated in the diabetic rat kidney and human proximal tubular epithelial cells treated with high glucose. Kidney international. 2003; 64:1012–1021. [PubMed: 12911551]
4. Escribano J, Hernando N, Ghosh S, Crabb J, Coca-Prados M. cDNA from human ocular ciliary epithelium homologous to beta ig-h3 is preferentially expressed as an extracellular protein in the corneal epithelium. Journal of cellular physiology. 1994; 160:511–521. [PubMed: 8077289]
5. Kannabiran C, Klintworth GK. TGFBI gene mutations in corneal dystrophies. Human mutation. 2006; 27:615–625. [PubMed: 16683255]
6. Price FW, Price MO. Adult keratoplasty: has the prognosis improved in the last 25 years? International ophthalmology. 2008; 28:141–146. [PubMed: 18196207]

7. Unal M, Arslan OS, Atalay E, Mangan MS, Bilgin AB. Deep anterior lamellar keratoplasty for the treatment of stromal corneal dystrophies. Cornea. 2013; 32:301–305. [PubMed: 22790186]
8. Vajpayee RB, Tyagi J, Sharma N, Kumar N, Jhanji V, Titiyal JS. Deep anterior lamellar keratoplasty by big-bubble technique for treatment corneal stromal opacities. American journal of ophthalmology. 2007; 143:954–957. [PubMed: 17434435]
9. Fagerholm P. Phototherapeutic keratectomy: 12 years of experience. Acta ophthalmologica Scandinavica. 2003; 81:19–32. [PubMed: 12631015]
10. Yao YF, Jin YQ, Zhang B, Zhou P, Zhang YM, Qiu WY, Mou SL, Wu LQ. Recurrence of lattice corneal dystrophy caused by incomplete removal of stroma after deep lamellar keratoplasty. Cornea. 2006; 25:S41–S46. [PubMed: 17001192]
11. Kim TI, Roh MI, Grossniklaus HE, Kang SJ, Hamilton SM, Schorderet DF, Lee WB, Kim EK. Deposits of transforming growth factor-beta-induced protein in granular corneal dystrophy type II after LASIK. Cornea. 2008; 27:28–32. [PubMed: 18245963]
12. Aldave AJ, Sonmez B, Forstot SL, Rayner SA, Yellore VS, Glasgow BJ. A clinical and histopathologic examination of accelerated TGFBIp deposition after LASIK in combined granular-lattice corneal dystrophy. American journal of ophthalmology. 2007; 143:416–419. [PubMed: 17317389]
13. Chiti F, Dobson CM. Amyloid formation by globular proteins under native conditions. Nature chemical biology. 2009; 5:15–22. [PubMed: 19088715]
14. Jahn TR, Makin OS, Morris KL, Marshall KE, Tian P, Sikorski P, Serpell LC. The common architecture of cross-beta amyloid. Journal of molecular biology. 2010; 395:717–727. [PubMed: 19781557]
15. Yuan C, Berscheit HL, Huang AJ. Identification of an amyloidogenic region on keratoepithelin via synthetic peptides. FEBS letters. 2007; 581:241–247. [PubMed: 17207483]
16. Lakshminarayanan R, Vithana EN, Chai SM, Chaurasia SS, Saraswathi P, Venkatraman A, Rojare C, Venkataraman D, Tan D, Aung T, Beuerman RW, Mehta JS. A novel mutation in transforming growth factor-beta induced protein (TGFbetaIp) reveals secondary structure perturbation in lattice corneal dystrophy. The British journal of ophthalmology. 2011; 95:1457–1462. [PubMed: 21835759]
17. Dighiero P, Drunat S, Ellies P, D'Hermies F, Savoldelli M, Legeais JM, Renard G, Delpech M, Grateau G, Valleix S. A new mutation (A546T) of the betaig-h3 gene responsible for a French lattice corneal dystrophy type IIIA. American journal of ophthalmology. 2000; 129:248–251. [PubMed: 10682981]
18. Stock EL, Feder RS, O'Grady RB, Sugar J, Roth SI. Lattice corneal dystrophy type IIIA. Clinical and histopathologic correlations. Archives of ophthalmology. 1991; 109:354–358. [PubMed: 2003794]
19. Runager K, Basaiawmoit RV, Deva T, Andreasen M, Valnickova Z, Sorensen CS, Karring H, Thogersen IB, Christiansen G, Underhaug J, Kristensen T, Nielsen NC, Klintworth GK, Otzen DE, Enghild JJ. Human phenotypically distinct TGFBI corneal dystrophies are linked to the stability of the fourth FAS1 domain of TGFBIp. The Journal of biological chemistry. 2011; 286:4951–4958. [PubMed: 21135107]
20. Karring H, Runager K, Thogersen IB, Klintworth GK, Hojrup P, Enghild JJ. Composition and proteolytic processing of corneal deposits associated with mutations in the TGFBI gene. Experimental eye research. 2012; 96:163–170. [PubMed: 22155582]
21. Poulsen ET, Runager K, Risor MW, Dyrlund TF, Scavenius C, Karring H, Praetorius J, Vorum H, Otzen DE, Klintworth GK, Enghild JJ. Comparison of two phenotypically distinct lattice corneal dystrophies caused by mutations in the transforming growth factor beta induced (TGFBI) gene. Proteomics. Clinical applications. 2014; 8:168–177. [PubMed: 24302499]
22. Karring H, Poulsen ET, Runager K, Thogersen IB, Klintworth GK, Hojrup P, Enghild JJ. Serine protease HtrA1 accumulates in corneal transforming growth factor beta induced protein (TGFBIp) amyloid deposits. Molecular vision. 2013; 19:861–876. [PubMed: 23592924]
23. Runager K, Garcia-Castellanos R, Valnickova Z, Kristensen T, Nielsen NC, Klintworth GK, Gomis-Ruth FX, Enghild JJ. Purification, crystallization and preliminary X-ray diffraction of wild-type and mutant recombinant human transforming growth factor beta-induced protein (TGFBIp).

Acta crystallographica. Section F, Structural biology and crystallization communications. 2009; 65:299–303. [PubMed: 19255489]

24. Reed SE, Staley EM, Mayginnes JP, Pintel DJ, Tullis GE. Transfection of mammalian cells using linear polyethylenimine is a simple and effective means of producing recombinant adeno-associated virus vectors. Journal of virological methods. 2006; 138:85–98. [PubMed: 16950522]
25. Bury AF. Analysis of Protein and Peptide Mixtures - Evaluation of 3 Sodium Dodecyl Sulfate-Polyacrylamide Gel-Electrophoresis Buffer Systems. J Chromatogr. 1981; 213:491–500.
26. Matsudaira P. Sequence from picomole quantities of proteins electroblotted onto polyvinylidene difluoride membranes. The Journal of biological chemistry. 1987; 262:10035–10038. [PubMed: 3611052]
27. Wales TE, Engen JR. Hydrogen exchange mass spectrometry for the analysis of protein dynamics. Mass spectrometry reviews. 2006; 25:158–170. [PubMed: 16208684]
28. Kussmann M, Nordhoff E, Rahbek-Nielsen H, Haebel S, Rossel-Larsen M, Jakobsen L, Gobom J, Mirgorodskaya E, KrollKristensen A, Palm L, Roepstorff P. Matrix-assisted laser desorption/ionization mass spectrometry sample preparation techniques designed for various peptide and protein analytes. J Mass Spectrom. 1997; 32:593–601.
29. Runager K, Klintworth GK, Karring H, Enghild JJ. The insoluble TGFBIp fraction of the cornea is covalently linked via a disulfide bond to type XII collagen. Biochemistry. 2013; 52:2821–2827. [PubMed: 23556985]
30. Karring H, Runager K, Valnickova Z, Thogersen IB, Moller-Pedersen T, Klintworth GK, Enghild JJ. Differential expression and processing of transforming growth factor beta induced protein (TGFBIp) in the normal human cornea during postnatal development and aging. Experimental eye research. 2010; 90:57–62. [PubMed: 19788893]
31. Andreasen M, Nielsen SB, Runager K, Christiansen G, Nielsen NC, Enghild JJ, Otzen DE. Polymorphic fibrillation of the destabilized fourth fasciclin-1 domain mutant A546T of the Transforming growth factor-beta-induced protein (TGFBIp) occurs through multiple pathways with different oligomeric intermediates. The Journal of biological chemistry. 2012; 287:34730–34742. [PubMed: 22893702]
32. Yang J, Han X, Huang D, Yu L, Zhu Y, Tong Y, Zhu B, Li C, Weng M, Ma X. Analysis of TGFBI gene mutations in Chinese patients with corneal dystrophies and review of the literature. Molecular vision. 2010; 16:1186–1193. [PubMed: 20664689]
33. Takacs L, Boross P, Tozser J, Modis L Jr, Toth G, Berta A. Transforming growth factor-beta induced protein, betaIG-H3, is present in degraded form and altered localization in lattice corneal dystrophy type I. Experimental eye research. 1998; 66:739–745. [PubMed: 9657906]
34. Klintworth GK, Valnickova Z, Enghild JJ. Accumulation of beta ig-h3 gene product in corneas with granular dystrophy. The American journal of pathology. 1998; 152:743–748. [PubMed: 9502416]
35. Korvatska E, Henry H, Mashima Y, Yamada M, Bachmann C, Munier FL, Schorderet DF. Amyloid and non-amyloid forms of 5q31-linked corneal dystrophy resulting from kerato-epithelin mutations at Arg-124 are associated with abnormal turnover of the protein. The Journal of biological chemistry. 2000; 275:11465–11469. [PubMed: 10753964]
36. Stix B, Leber M, Bingemer P, Gross C, Ruschoff J, Fandrich M, Schorderet DF, Vorwerk CK, Zacharias M, Roessner A, Rocken C. Hereditary lattice corneal dystrophy is associated with corneal amyloid deposits enclosing C-terminal fragments of keratoepithelin. Investigative ophthalmology & visual science. 2005; 46:1133–1139. [PubMed: 15790870]
37. Hedegaard CJ, Thogersen IB, Enghild JJ, Klintworth GK, Moller-Pedersen T. Transforming growth factor beta induced protein accumulation in granular corneal dystrophy type III (Reis-Bucklers dystrophy). Identification by mass spectrometry in 15 year old two-dimensional protein gels. Molecular vision. 2003; 9:355–359. [PubMed: 12942051]
38. Grothe HL, Little MR, Sjogren PP, Chang AA, Nelson EF, Yuan C. Altered protein conformation and lower stability of the dystrophic transforming growth factor beta-induced protein mutants. Molecular vision. 2013; 19:593–603. [PubMed: 23559853]
39. Underhaug J, Koldso H, Runager K, Nielsen JT, Sorensen CS, Kristensen T, Otzen DE, Karring H, Malmendal A, Schiott B, Enghild JJ, Nielsen NC. Mutation in transforming growth factor beta

induced protein associated with granular corneal dystrophy type 1 reduces the proteolytic susceptibility through local structural stabilization. Biochimica et biophysica acta. 2013; 1834:2812–2822. [PubMed: 24129074]

40. Nazabal A, Hornemann S, Aguzzi A, Zenobi R. Hydrogen/deuterium exchange mass spectrometry identifies two highly protected regions in recombinant full-length prion protein amyloid fibrils. J Mass Spectrom. 2009; 44:965–977. [PubMed: 19283723]
41. French KC, Makhatadze GI. Core sequence of PAPf39 amyloid fibrils and mechanism of pH-dependent fibril formation: the role of monomer conformation. Biochemistry. 2012; 51:10127–10136. [PubMed: 23215256]
42. Yamaguchi K, Katou H, Hoshino M, Hasegawa K, Naiki H, Goto Y. Core and heterogeneity of beta2-microglobulin amyloid fibrils as revealed by H/D exchange. Journal of molecular biology. 2004; 338:559–571. [PubMed: 15081813]
43. Carulla N, Caddy GL, Hall DR, Zurdo J, Gairi M, Feliz M, Giralt E, Robinson CV, Dobson CM. Molecular recycling within amyloid fibrils. Nature. 2005; 436:554–558. [PubMed: 16049488]
44. Sanchez L, Madurga S, Pukala T, Vilaseca M, Lopez-Iglesias C, Robinson CV, Giralt E, Carulla N. Abeta40 and Abeta42 amyloid fibrils exhibit distinct molecular recycling properties. J Am Chem Soc. 2011; 133:6505–6508. [PubMed: 21486030]
45. Tjernberg LO, Lilliehook C, Callaway DJ, Naslund J, Hahne S, Thyberg J, Terenius L, Nordstedt C. Controlling amyloid beta-peptide fibril formation with protease-stable ligands. The Journal of biological chemistry. 1997; 272:12601–12605. [PubMed: 9139713]
46. Tjernberg LO, Naslund J, Lindqvist F, Johansson J, Karlstrom AR, Thyberg J, Terenius L, Nordstedt C. Arrest of beta-amyloid fibril formation by a pentapeptide ligand. The Journal of biological chemistry. 1996; 271:8545–8548. [PubMed: 8621479]
47. Gordon DJ, Sciarretta KL, Meredith SC. Inhibition of beta-amyloid(40) fibrillogenesis and disassembly of beta-amyloid(40) fibrils by short beta-amyloid congeners containing N-methyl amino acids at alternate residues. Biochemistry. 2001; 40:8237–8245. [PubMed: 11444969]
48. Findeis MA, Musso GM, Arico-Muendel CC, Benjamin HW, Hundal AM, Lee JJ, Chin J, Kelley M, Wakefield J, Hayward NJ, Molineaux SM. Modified-peptide inhibitors of amyloid beta-peptide polymerization. Biochemistry. 1999; 38:6791–6800. [PubMed: 10346900]
49. Bett CK, Serem WK, Fontenot KR, Hammer RP, Garno JC. Effects of peptides derived from terminal modifications of the abeta central hydrophobic core on abeta fibrillization. ACS chemical neuroscience. 2010; 1:661–678. [PubMed: 22778807]
50. Wei CW, Peng Y, Zhang L, Huang Q, Cheng M, Liu YN, Li J. Synthesis and evaluation of ferrocenoyl pentapeptide (Fc-KLVFF) as an inhibitor of Alzheimer's Abeta(1)-(4)(2) fibril formation in vitro. Bioorganic & medicinal chemistry letters. 2011; 21:5818–5821. [PubMed: 21855336]
51. Ladiwala AR, Bhattacharya M, Perchiacca JM, Cao P, Raleigh DP, Abedini A, Schmidt AM, Varkey J, Langen R, Tessier PM. Rational design of potent domain antibody inhibitors of amyloid fibril assembly. Proceedings of the National Academy of Sciences of the United States of America. 2012; 109:19965–19970. [PubMed: 23161913]

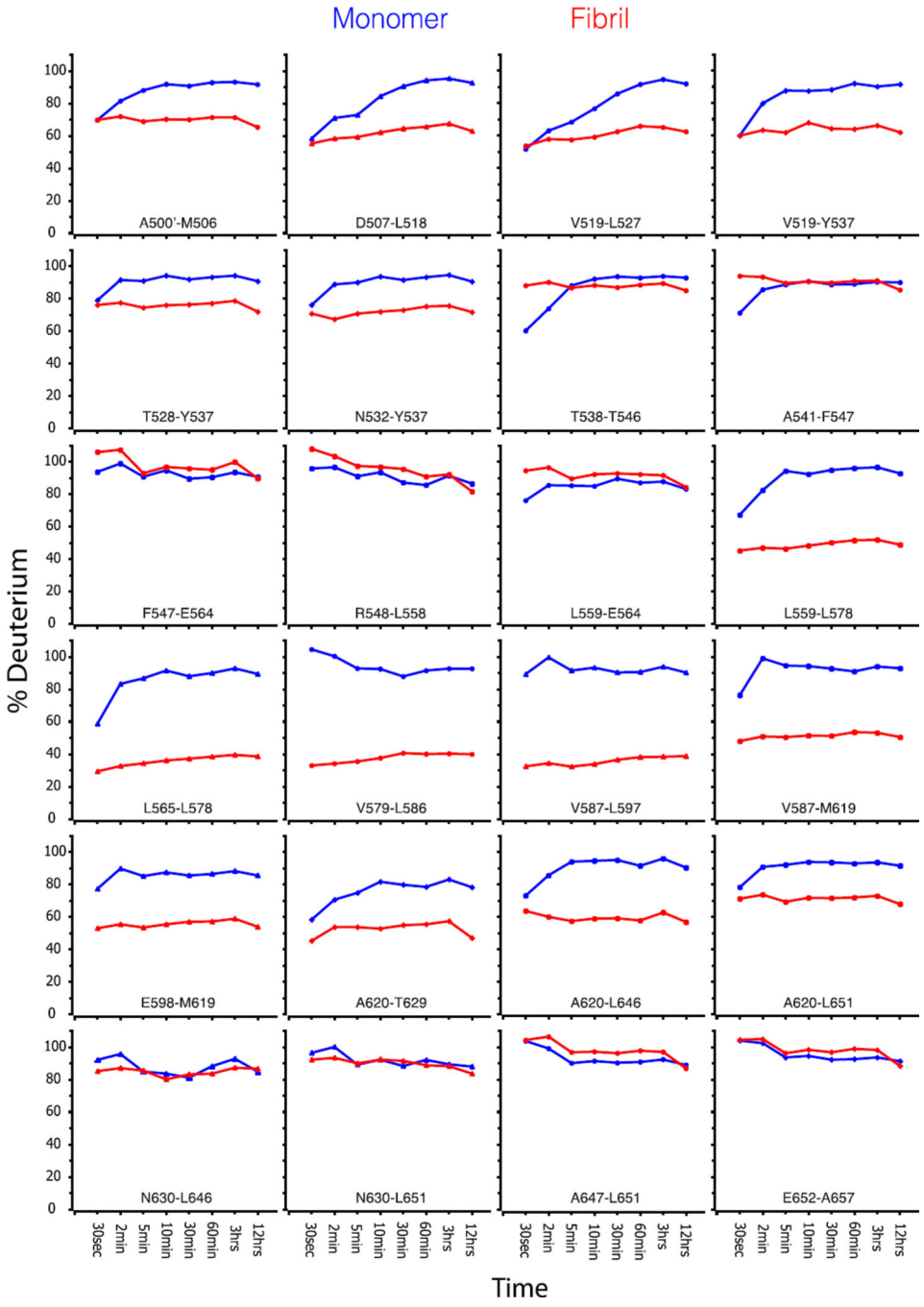

Figure 1.

Fibril formation lowers the hydrogen-deuterium exchange rate of two regions in A546T FAS1-4. HDX-MS analysis measured the hydrogen exchange rate of fibrillated (red) and monomeric A546T FAS1-4 (blue). The samples were allowed to exchange hydrogens from 30 sec up to 12 h, followed by quenching and proteolysis with pepsin. Each diagram shows the degree of deuterium exchange relative to a fully deuterated monomer. Peptides covering the entire sequence of A546T FAS1-4 are shown. The peptides covering the region L565-

L597 showed a high degree of protection from the solvent in the fibrils, while the regions A500'-Y537 and E598-T629 displayed less protection.

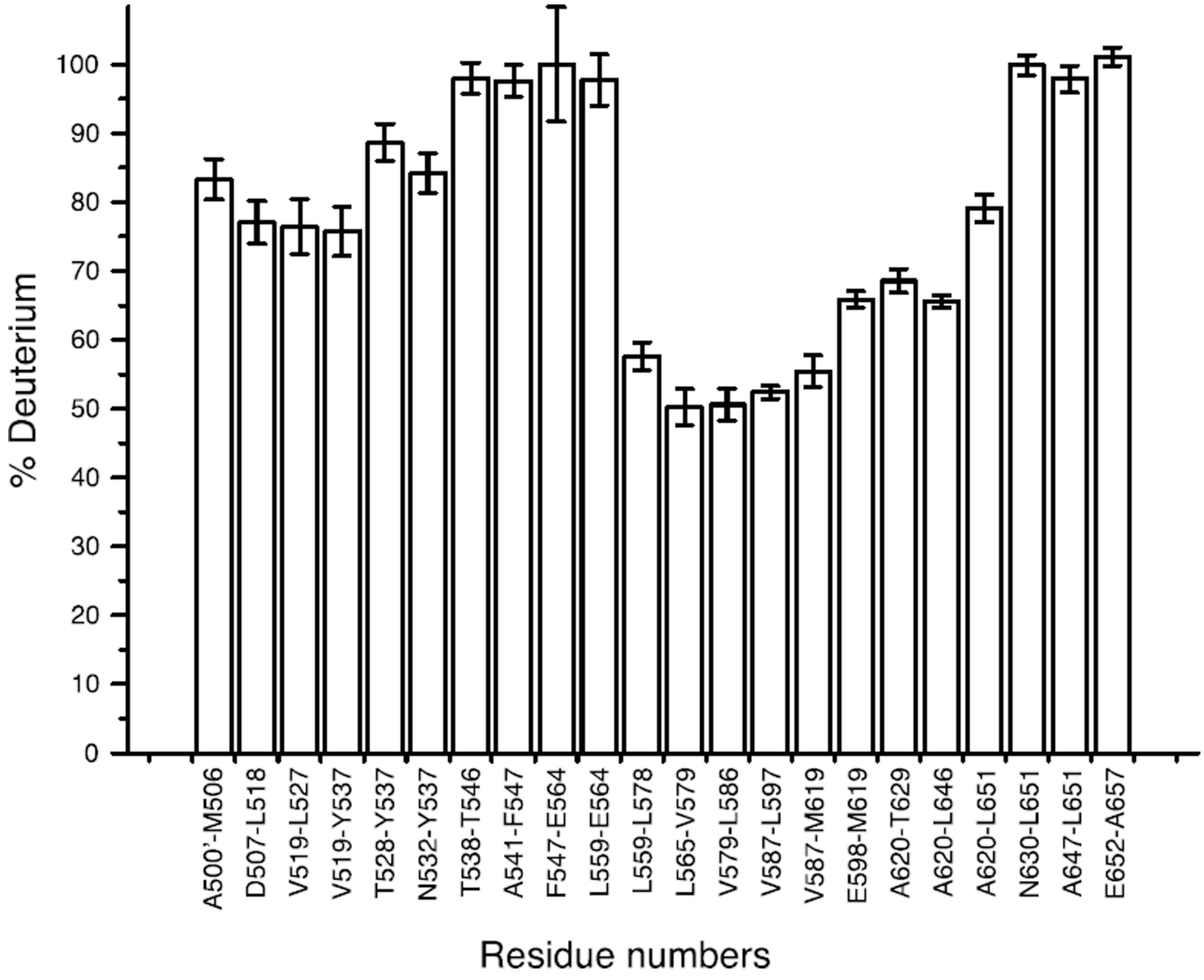

Figure 2.

The A546T FAS1-4 fibril core is stable over prolonged periods of time. The level of resistance towards hydrogen deuterium exchange in fibrillated A546T FAS1-4 was tested by prolonged incubation in deuterated buffer. The fibrils were allowed to exchange hydrogens for 72 h, followed by quenching and proteolysis with pepsin. Each bar represents the deuterium uptake of a peptic peptide relative to a fully deuterated monomer. The data represent the average deuterium uptake of three replicates. Error bars denote standard deviations.

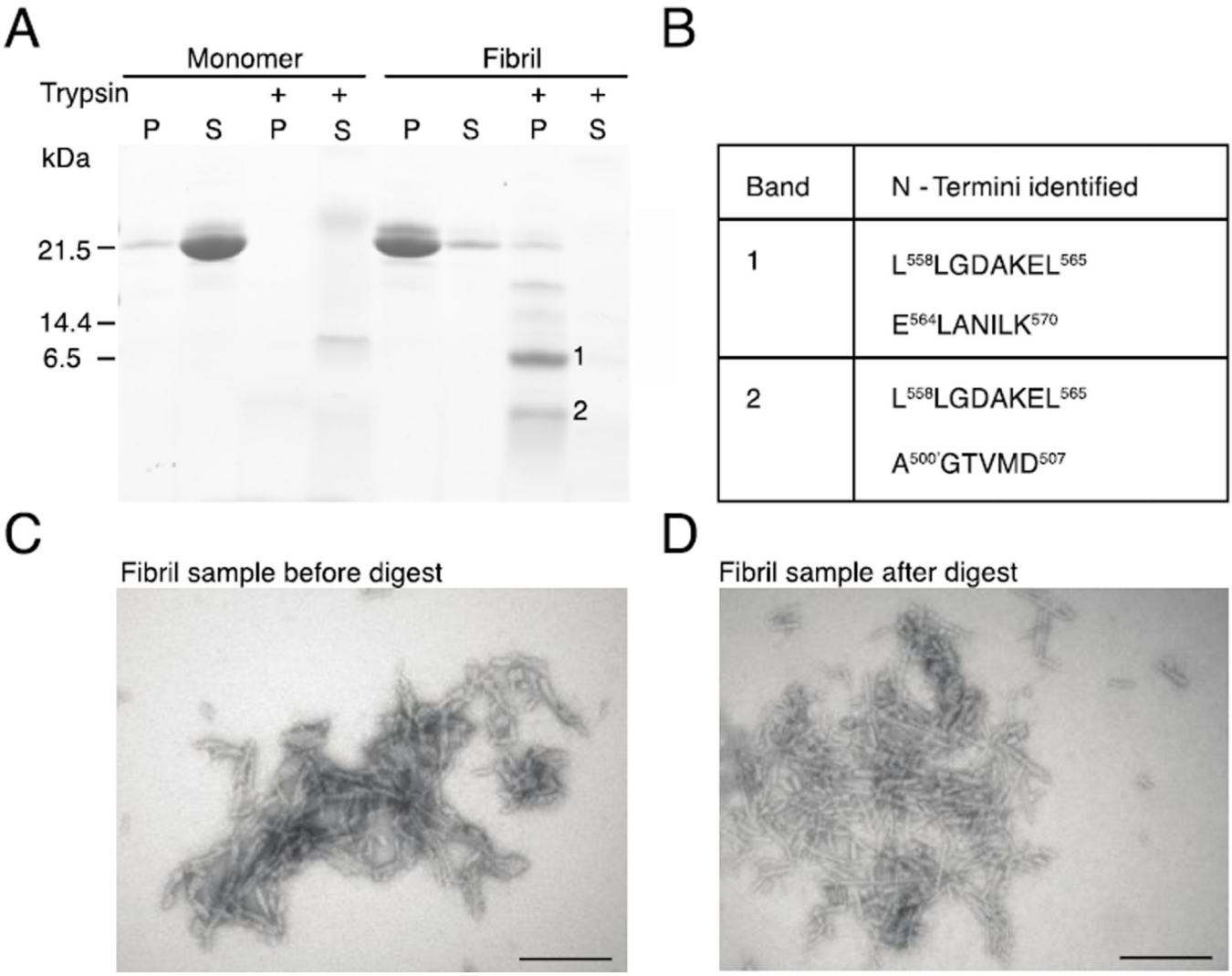

Figure 3.

The amyloid structure protects two regions of A546T FAS1-4 against proteolytic degradation. *A*, Monomeric and fibrillated A546T FAS1-4 were divided into a supernatant (S) and pellet (P) fractions using centrifugation and subsequently analyzed using SDS-PAGE. The majority of monomeric A546T FAS1-4 was in the supernatant, and fibrillated A546T FAS1-4 was located in the pellet. The isolated monomeric A546T FAS1-4 (supernatant) and fibrillated sample (pellet) were digested with trypsin and again separated into pellets and supernatants using centrifugation. Monomeric A546T FAS1-4 is easily digestible with trypsin, but the fibrillated sample contains smaller, insoluble fragments (marked 1 and 2). *B*, N-termini identified in bands (bands marked 1 and 2) from SDS-PAGE. *C*, Electron microscopy of the undigested A546T FAS1-4 fibril pellet showing fibrils that are relatively short, straight and unbranched, but somewhat irregular. *D*, Electron microscopy of the A546T FAS1-4 fibril pellet after trypsin digest, confirms that part of the fibril structure remains intact after proteolysis. The scale bars denote 200 nm.

A

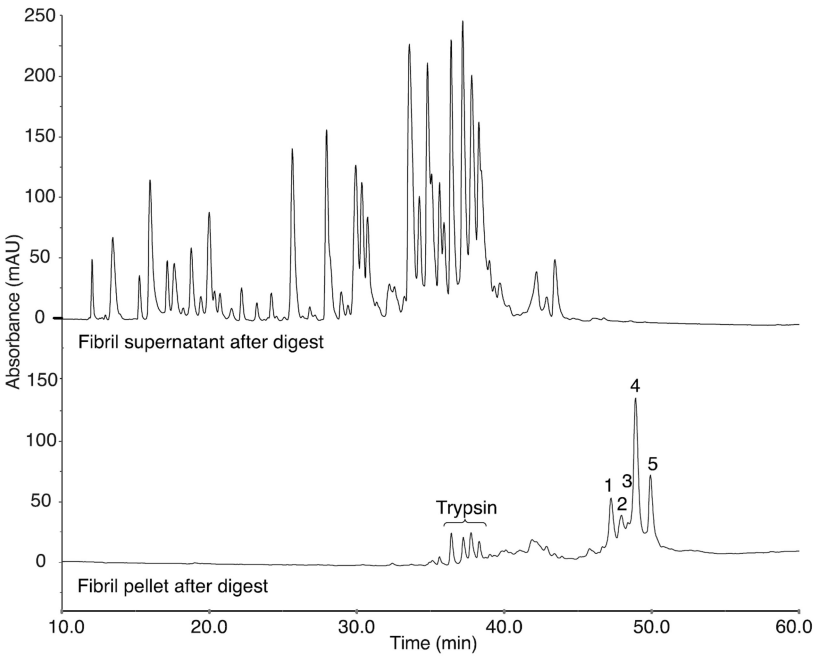

B

Peak	N-termini identified	Obs. mass (MH+) /Da	Exp. mass (MH+) /Da	Region covered	No. of missed cleavages
1	ELANILKY	8522.684	8521.74	E564-K642	6
2	LLGDAKEL	4789.150	4789.59	L558-K602	5
3	AGMGTVMD	3566.270	3566.81	A500'-R533	2
4	LLGDAKEL	9119.072	9119.44	L558-R642	7
5	AGMGTVMD	5282.857	5281.97	A500'-R548	3

C

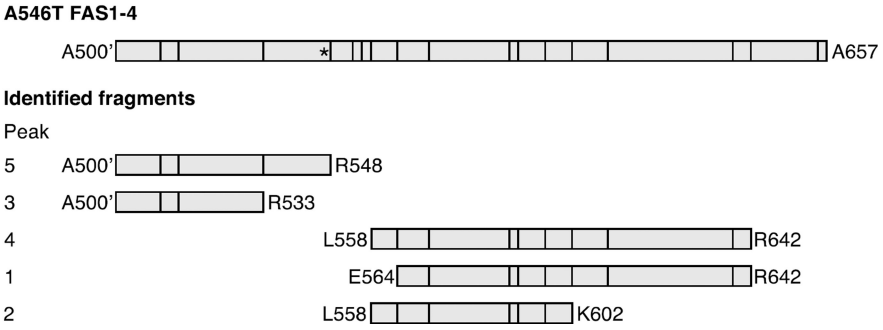

Figure 4.

Isolation of trypsin-generated fragments that represent the fibril core region. Fibrillated A546T FAS1-4 was treated with trypsin at a ratio of 1:1 w/w and separated into pellet and supernatant fractions. *A*, Chromatograms from RP-HPLC of the pellet (lower chromatogram) and supernatant (upper chromatogram) fractions. Five peaks (marked 1–5), representing the fibril core, were specifically retained in the pellet fraction, and four minor peaks corresponded to peptides from the high amount of trypsin added (data not shown). *B*, N-terminal sequencing and mass spectrometry analyses determined the sequences of the five

peptides that covered the fibril core region. The table contains the identified N-termini, observed masses, expected masses, regions covered in A546T FAS1-4, and the number of missed trypsin cleavages. *C*, Schematic representation of the identified fibril core fragments with vertical lines representing potential trypsin cleavage sites and an asterisk marking the A546T mutation site.

A

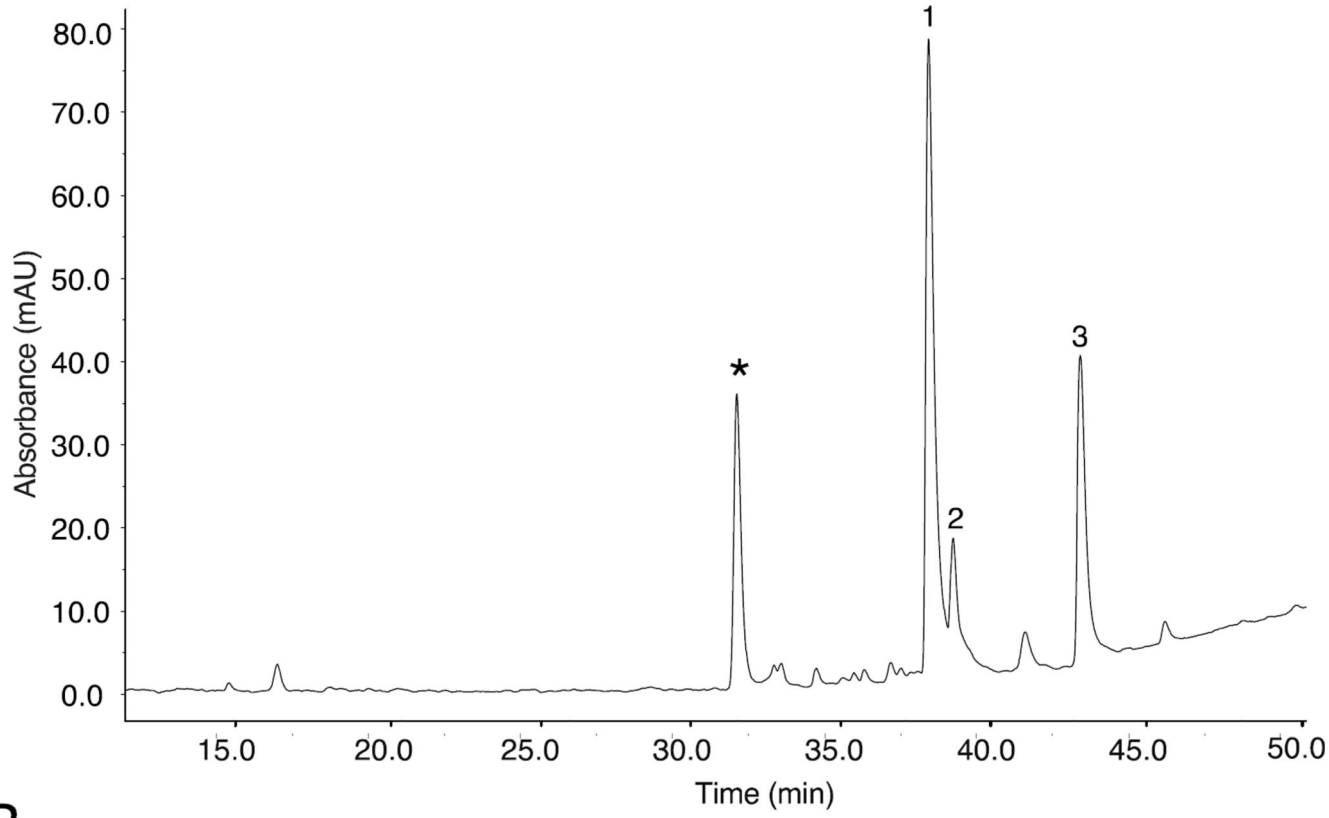

B

Peak	N-Termini Identified	Obs. mass (MH+) /Da*	Exp. mass (MH+) /Da	Region Covered
1	YHIGDEIL	1869.01	1869.02	Y571-R588
2	YHIGDEIL FSMLVAAI	1869.03 -	- -	Not determined
3	FSMLVAAI	2022.07 2038.07	2022.07 2038.07	F515-R533 F515-R533 (+O)

Figure 5.

Two tryptic peptides of A546T FAS1-4 are highly insoluble. Fibrillation of tryptic peptides of A546T FAS1-4 reveals two aggregation prone peptides in the pellet fraction. *A*, After extensive trypsin degradation and subsequent fibrillation, the tryptic peptides from A546T FAS1-4 were separated into a pellet fraction and a supernatant fraction. The aggregated peptides in the pellet fraction were separated using RP-HPLC, and four major peaks were observed. The peak marked with an asterisk did not contain any peptide detected by N-terminal sequencing or mass spectrometry. *B*, Table of identified N-termini and observed masses from the three peaks in panel *A* and with expected masses and regions covered in A546T FAS1-4.

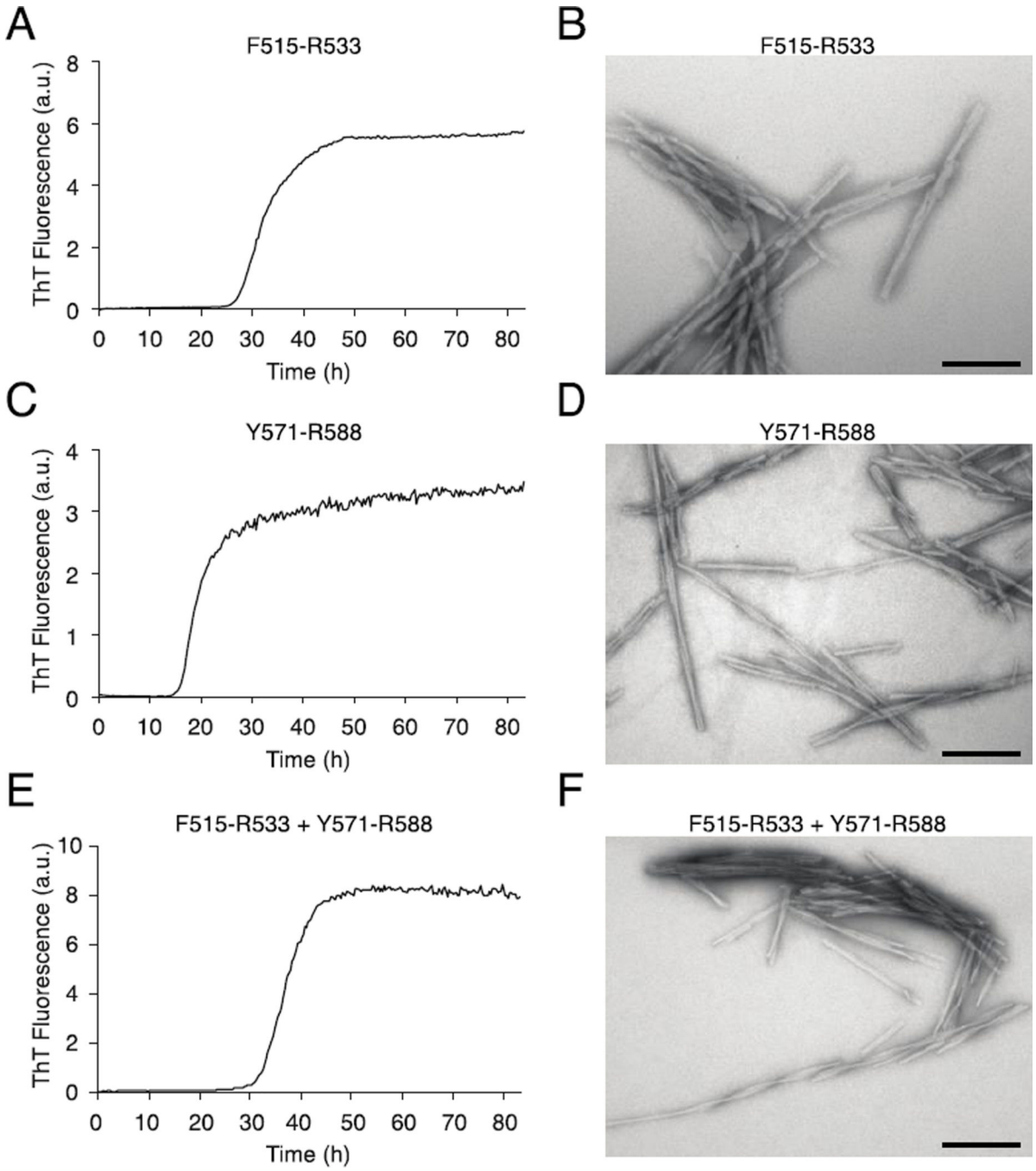

Figure 6.

The ThT fluorescence assay confirms the fibrillating propensity of the two fibril core peptides. The fibril formation of the F515-R533 and Y571-R588 peptides alone and mixed together was followed using ThT fluorescence, and the end products were visualized using TEM. *A*, Fibrillation of the peptide F515-R533 visualized using ThT fluorescence reveals a lag phase of approximately 25 h, followed by an increase in fluorescence, after which time the end level of ThT fluorescence was reached. *B*, TEM imaging of the fibrils formed by F515-R533 revealed straight, unbranched, and relatively long fibrils that were packed in

bundles. *C*, Fibrillation of the Y571-R588 peptide followed by ThT fluorescence. Fibrillation of the Y571-R588 peptide had a lag phase of approximately 15 h followed by a steep increase in fluorescence, after which time the end level of ThT fluorescence was quickly reached. *D*, TEM imaging of the fibrils of Y571-R588 reveals straight, long fibrils, including some fibrils with a twist. However, fewer fibrils are observed in bundles compared with F515-R533. *E*, Equimolar amounts of F151-R533 and Y571-R588 were incubated in the presence of ThT. A lag time of 30 h was observed. *F*, TEM image shows straight fibrils with higher order structures and twists. The scale bars denote 200 nm.

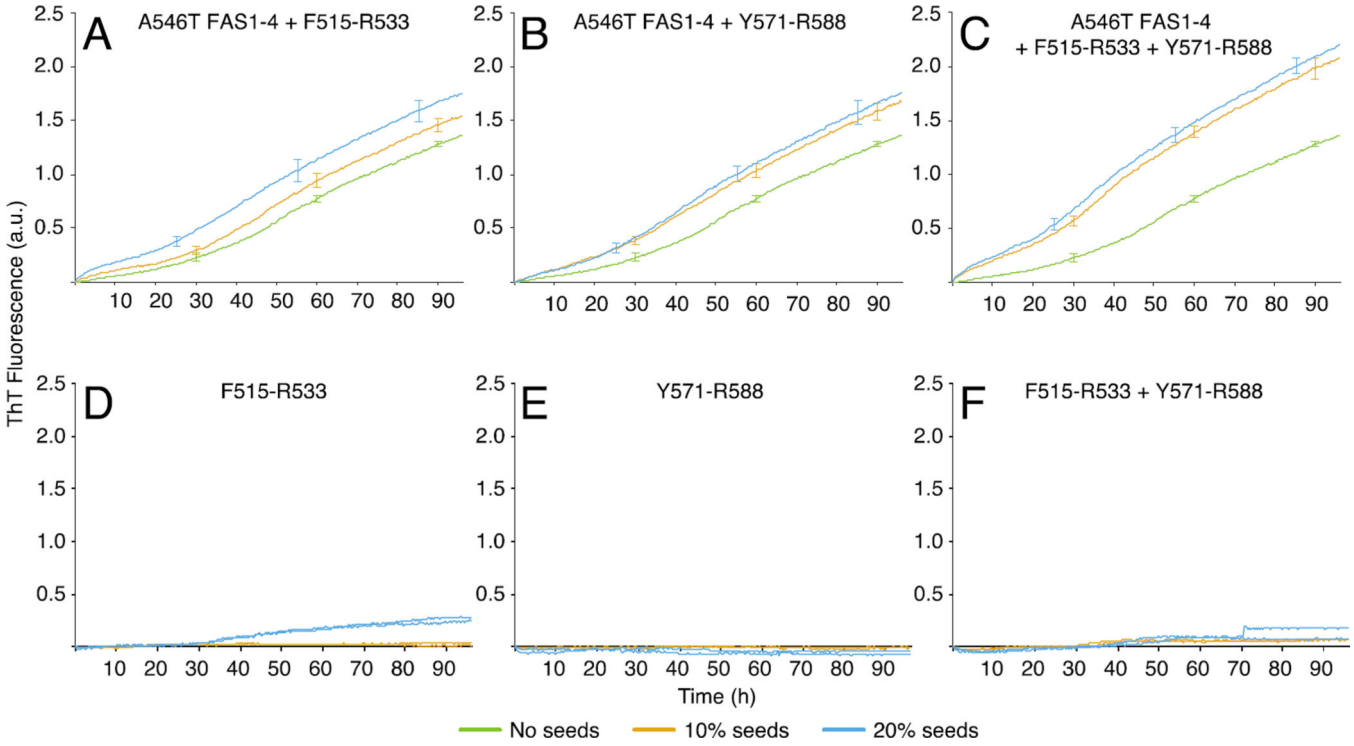

Figure 7.

Seeds of the fibril core peptides induce fibrillation of A546T FAS1-4. The propensity of the two core peptides to seed fibrillation of A546T FAS1-4 was analyzed using ThT fluorescence assay. *A–C*, Averaged fibrillation curves (n = 3) representing A546T FAS1-4 alone and in combination with 10% or 20% fibril seeds of the core peptides alone or in combination incubated for 96 h. Error bars denote the standard deviations. *D-F*, Seeds of each core peptide alone or in combination incubated in the absence of A564T FAS1-4 (duplicate experiments). The data shows that seeds of both the F515-R533 and the Y571-R588 peptides are able to seed the fibrillation of A546T FAS1-4 in a dose-dependent manner. When A546T FAS1-4 was incubated with seeds of the mixed peptides an enhanced effect was observed. None of the observed effects could be attributed to a background signal for the peptide seeds since the increase in ThT fluorescence observed for the seeds alone (*D–F*) displayed a progression distinct from of those of the seeding experiments.

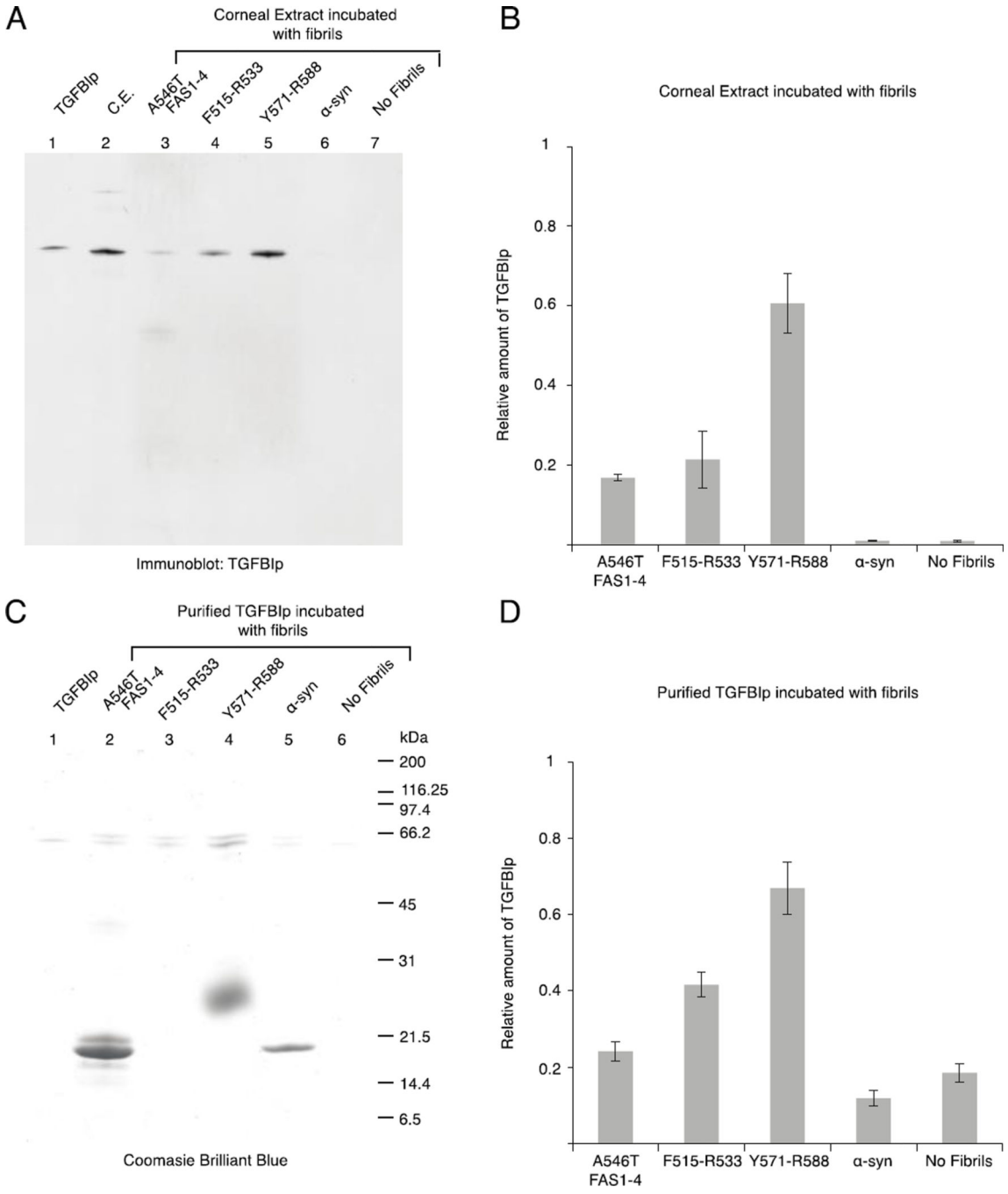

Figure 8.

WT TGFBIp aggregation is induced by fibril seeds of the core peptides. Corneal extract (*A*) or recombinant TGFBIp (*C*) were incubated with fibrillated samples of A546T FAS1-4, F515-R533, Y571-R588, α-synuclein, or no fibrils. Subsequently, the fibrils and interaction partners were extensively washed, and the proteins were resolved using SDS-PAGE. *A*, The proteins from the corneal extract were visualized by immunoblotting using anti-TGFBIp polyclonal antiserum. Purified TGFBIp and corneal extract (C.E.) were included as controls. *B*, Relative amount of TGFBIp from the corneal extract bound to the fibrils, n = 3, error bars

= standard deviation. *C*, Purified recombinant TGFBIp was visualized using Coomassie brilliant blue staining. Recombinant TGFBIp was included as a control. F515-R533 migrated with the dye front, and therefore, it is not visible on the gel (Lane 3); Y571-R588 migrated above its size as a very fuzzy band (Lane 4). *D*, Relative amount of purified TGFBIp bound to the fibrils, n = 3, error bars represent the standard deviation. Both corneal TGFBIp and recombinant TGFBIp aggregate in the presence of fibrillated core peptides, with Y571-R588 causing the highest degree of aggregation.

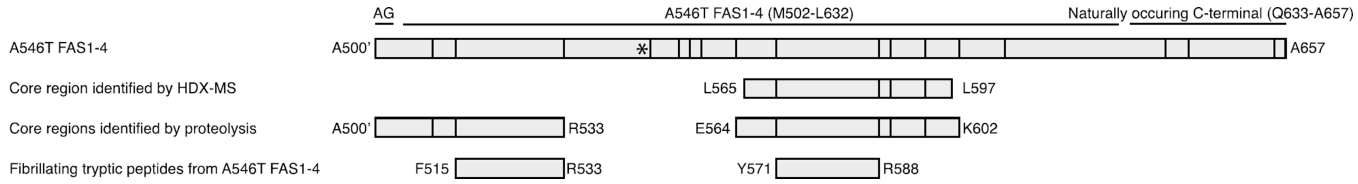

Figure 9.

Schematic representation of identified core regions in A546T FAS1-4. Linear representation of the A546T FAS1-4 domain, including the N-terminally added residues AG and the naturally occurring C-terminal. Tryptic cleavage sites are represented by lines, and the mutational site of A546T is represented by an asterisk. The fibril core regions identified by HDX-MS and proteolysis are depicted along with the two fibrillating tryptic peptides from A546T FAS1-4, F515-R533 and Y571-R588.